XAS, ESR and Potentiometric Studies of Three Dinuclear *N,N′-para*-Xylylenebis(tetraazamacrocycle)copper(II) Complexes − X-ray Crystal Structure of [*N,N′-p*-Xylylenebis(cyclen)]copper(II)

Mathieu Soibinet,[a] Isabelle Déchamps-Olivier,*[a] Emmanuel Guillon,[a] Jean-Pierre Barbier,[a] Michel Aplincourt,[a] Françoise Chuburu,[b] Michel Le Baccon,[b] and Henri Handel[b]

Keywords: Copper / ESR spectroscopy / Macrocyclic ligands / Potentiometry / X-ray studies

Dicopper complexes with *N,N′-p*-xylylenebis(cyclam or cyclen) and with the heteroditopic *N,N′-p*-xylylenebis(cyclam-cyclen) were synthesized. An X-ray study of the *N,N′-p*-xylylenebis(cyclen)dicopper complex showed that the copper(II) ion is five-coordinate with an H_2O molecule in apical position. With this ligand, a polymeric chain was also obtained in the presence of KSCN. The terminal donor atoms of the bridging NCS^- anion are coordinated in apical position to the square-pyramidal copper(II) ion. Two alternating kinds of Cu_2L^{4+} moieties are present in the chain, the first with two N_4S chromophores and the second with two N_5 chromophores. EXAFS and XANES results are in agreement with a five-coordinate copper ion in the cyclen unit and a six-coordinate copper ion in the cyclam unit. Thermodynamic constants were determined by potentiometry. The existence of dinuclear Cu_2L^{4+} species (ligand/metal ratio < 1) and mononuclear $CuLH_n^{(2+n)+}$ species (ligand/metal ratio > 1) were confirmed by an ESR study at variable pH.

Introduction

Since the early 1960s, homodinuclear macrocyclic complexes have been studied extensively.[1] The interest in such dinuclear complexes stems from different particularities. Fundamentally, the presence of two metal centres not too far away from one another can induce interactions that can influence the complex's magnetic or redox properties. These complexes have been used in the development of two-centred metal catalytic reagents.[2] Moreover, these dimacrocyclic complexes may serve as models for the charge transfer, electron transport, and allosteric behaviour found in many metal-containing biochemical systems.[3,4] Besides their fundamental interest, these ligands and complexes are also used in anti-HIV drugs, in particular, the *m*- or *p*-xylylenebis(cyclam)[5−7] (referred to as AMD 2986 and AMD 3100, respectively) and the *p*-xylylenebis(cyclen)dizinc complexes[8] are implicated in the inhibition of particular HIV strains with low levels of cytotoxicity.

The coordination of bis(macrocycles) containing two covalently, potentially chelating subunits has been studied intensively in recent years.[9] Cyclam and cyclen are involved in compounds with linkages between two nitrogen atoms or two carbon atoms. The bridge (alkanediyl chain or xylylene group) can modify the intermetallic distance and the orientation of the macrocyclic ring. Our purpose is the investigation of the copper(II) coordination with the little studied *p*-xylylenebis(*N,N′*-cyclam) or -bis(*N,N′*-cyclen) (Scheme 1).

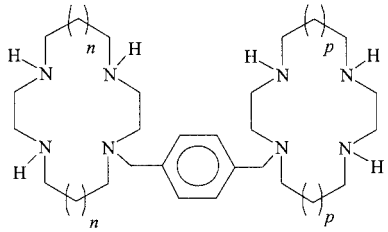

*para*cyclen	$n = p = 0$
*para*cyclam-cyclen	$n = 1$ and $p = 0$
*para*cyclam	$n = p = 1$

Scheme 1

Except for the dizinc complex used in anti-HIV drugs, the metal complexes with these ligands have seldom been studied. With the *p*-xylylenebis(tetraazamacrocycles) ligands, the copper complexes have been described; Fabbrizzi et al.[10] only studied the mutual copper interaction by electrochemistry, while the intermetallic distances were esti-

[a] GRECI, Université de Reims Champagne-Ardenne, B. P. 1039, 51687 Reims Cedex 2, France
Fax: (internat.) + 33-3/26913243
E-mail: isabelle.dechamps@univ-reims.fr
[b] UMR CNRS 6521, Université de Bretagne Occidentale, B. P. 809, 29285 Brest Cedex, France

  DOI: 10.1002/ejic.200200517

mated by Guilard et al.[11] by ESR spectroscopy. These authors demonstrated the influence of different spacers linked to the two macrocycles on the electrochemical properties and on the Cu−Cu distances in these bis(tetraazamacrocycle) complexes. In addition, electrochemical aqueous solution studies and UV/Vis and ESR spectroscopic investigations have been carried out on other (tetraazamacrocycle)copper complexes such as bis(isocyclam)[12] and spirocyclam.[13] Kinetic phenomena are always present when a metallic ion is incorporated in a tetraazamacrocycle[14] or in the tetraaza units of a bis(macrocycle).[15] Solution studies therefore have to be performed carefully, taking the kinetic of complexation of the tetraaza rings into account. Crystallographic data for this type of compounds are very scarce, and to the best of our knowledge, only the structure of a dinuclear copper(II) complex with two 1,4,7,10-tetraazacyclododecane units *N,N′*-bridged by 2,6-dimethyl-1-methoxybenzene[16] has been described in the literature.

In order to understand the behaviour of a ligand implicated in anti-HIV drugs, it was interesting to investigate the complexation of these ligands with a biologically interesting cation such as copper(II). These studies were made by combining potentiometry and ESR spectra, and taking kinetic phenomena into account. A heteroditopic bis(macrocyclic) ligand was also studied (see Scheme 1, *para*cyclam-cyclen ligand). Solid compounds were also prepared, but only complexes with *para*cyclen give crystals suitable for X-ray studies. The structures of monomeric (*para*cyclen)$Cu_2(ClO_4)_4$ and polymeric $[(para\text{cyclen})Cu_2]_2(SCN)_8$ chains induced by the potentially bidentate thiocyanate anion, have been reported. XAS results permitted the determination of the environment around the copper cation when a cyclam unit is present in the ligand.

Results and Discussion

Solution Studies

Ligand Protonation Constants

Protometric study of the three ligands allowed us to determine the protonation constants given in Table 1.

For each ligand, the first four constants follow the usual order, their values decreasing from K_1 to K_4; for the last one (K_4), both macrocycles are diprotonated. As far as the values of the last four constants (K_5 to K_8) are concerned, only some of them could be calculated, the others being too weak to be given with sufficient accuracy. In the case of the ligand *para*cyclam-cyclen, one inversion among these constants' values is observed ($K_7 > K_5$ and K_6).

Such an inversion in the order of the values of protonation constants has been reported previously[18] for cyclam, K_4 being greater than K_3 (Table 1). We also determined the protonation constants of cyclam, and our values are in good agreement with those previously obtained[18] especially if we take the differences in experimental conditions (ionic strength, temperature) into account. The inversion of the K_3 and K_4 constant values was attributed to a conformational modification of the cyclam accompanying its third protonation.[18] Consequently, whereas the addition of the third proton is difficult because of energetic requirements accompanying to the geometrical change, the addition of the fourth one is facilitated.

The same interpretation can be proposed for the successive protonations of *para*cyclam-cyclen. Constants K_5 and K_6 correspond to the attachment of a third proton on each of the two cycles, whereas constant K_7 corresponds to the attachment of a fourth proton on the cyclam cycle. As with the cyclam, the third protonation is difficult, which explains why the constant value K_5 is below that of K_7.

Copper Complexation Studies

The complexation kinetics of the macrocycles cyclen and cyclam are well-known pH-dependent phenomena. As a result, the batch method is often used in order to study the formation of the complexes in solution. However, we did not use this method in our experiments, since it requires a large quantity of product. We thus performed classical titrations, all our measures being made after waiting times, at constant initial pH, of 60, 90, and 120 d between the preparation of the solutions and the beginning of the titrations. All the titrations gave identical results.

Protometric titrations in the presence of copper were monitored by ESR at 150 K. Whatever the pH of the solution may have been, for ratios R = [ligand]/[metal] greater than 1, ESR spectra each give a signal of four equidistant lines, characteristic of the presence of mononuclear species. The obtained spectroscopic parameters $g_{\|}$ and $A_{\|}$ are very close to those of complexes formed with cyclam or cyclen[19]

Table 1. Logarithms of successive protonation constants

	$\log K_1$ [a]	$\log K_2$	$\log K_3$	$\log K_4$	$\log K_5$	$\log K_6$	$\log K_7$	$\log K_8$
*para*cyclen	11.1 (0.1)	10.5 (0.1)	9.44 (0.04)	8.75 (0.06)				
*para*cyclam	12.3 (0.1)	11.1 (0.1)	9.80 (0.05)	8.9 (0.1)	2.90 (0.07)	ca. 1		
*para*cyclam-cyclen	12.5 (0.2)	10.95 (0.1)	9.7 (0.1)	8.86 (0.04)	2.76 (0.07)	1.7 (0.3)	2.9 (0.3)	
cyclen	11.13 (0.01)	10.17 (0.06)	1.51(0.09)					
cyclen[b]	10.97	9.87	< 2					
cyclam	11.72 (0.01)	10.57 (0.01)	1.91 (0.08)	2.7 (0.1)				
cyclam[c]	11.6	10.6	1.61	2.42				

[a] Values in parentheses represent 2σ standard deviation. $\log K_n$ refers to the equilibrium $LH_{n-1} + H^+ \leftarrow\!\!\rightarrow LH_n$. [b] Ref.[17] [c] Ref.[18]

Table 2. ESR parameters of copper complexes in aqueous solution

		$g_{\parallel}$	$A_{\parallel}$ [10^{-4} cm^{-1}]	$g_{\perp}$	$A_{\perp}$ [10^{-4} cm^{-1}]
*para*cyclen[a]	$CuLH_n^{(2+n)+}$	2.20	180	2.05	10
	Cu_2L^{4+}	2.19	92	2.06	10
*para*cyclam[a]	$CuLH_n^{(2+n)+}$	2.19	192	2.06	10
	Cu_2L^{4+}	2.19	95	2.06	10
*para*cyclam-cyclen[a]	$CuLH_n^{(2+n)+}$	2.19	192	2.06	10
	Cu_2L^{4+}	2.19	93	2.06	10
cyclen[b]	CuL^{2+}	2.198	184	2.057	24.1
cyclam[b]	CuL^{2+}	2.186	205	2.049	38.7

[a] Values obtained by simulation. [b] Ref.[19]

(Table 2). For ratios R smaller than 1, the obtained ESR spectra each show a signal with seven equidistant lines, characteristic of the formation of dinuclear species.[11] The values of the $g_{\parallel}$ parameter are identical to those of the previous complexes, whereas the values of $A_{\parallel}$ are half those obtained for mononuclear complexes (Table 2). The complexes formed are therefore different, given the experimental conditions of the preparation of the solutions, but the copper environments in mono- or dinuclear complexes are similar to those of the copper ion in the cyclen or the cyclam complexes.

The stability constants of the complexes were calculated, taking only mononuclear species into account for ratios R greater than 1, and only dinuclear species for ratios R less than 1. This is in agreement with the ESR study. The values of the global constants of formation are presented in Table 3.

Table 3. Logarithms of overall stability constants

	$CuLH_2^{4+}$ log β_{112} [a]	$CuLH^{3+}$ log β_{111}	CuL^{2+} log β_{110}	Cu_2L^{4+} log β_{210}
*para*cyclen	39.4 (0.4)	30.4 (0.4)	19.6 (0.2)	39.2 (0.3)
*para*cyclam	42.3 (0.1)	33.8 (0.3)	23.5 (0.5)	44.0 (0.3)
*para*cyclam-cyclen	42.4 (0.1)	33.7 (0.2)	22.3 (0.3)	42.3 (0.3)
cyclen[b]			23.3	
cyclam[b]			26.5	

[a] Values in parentheses represent 2σ standard deviation. [b] Ref.[17]

In the case of the dinuclear species Cu_2L^{4+}, on the one hand, the complexation of two copper(II) ions by the four nitrogen atoms of each cycle induces the complete deprotonation of the ligand. On the other hand, in the case of mononuclear complexes $CuLH_n^{(n+2)+}$, the copper ion is engaged only in one macrocycle, and we obtain three complexation constants, corresponding to the formation of $CuLH_2^{4+}$ and then to the deprotonation of two nitrogen atoms from the non-complexed cycle (see distribution curves Figure 1).

The stability constants obtained are all very high, so the complexes formed are very stable. The values of the logarithms of the constants β_{110} of the complexes CuL^{2+} formed

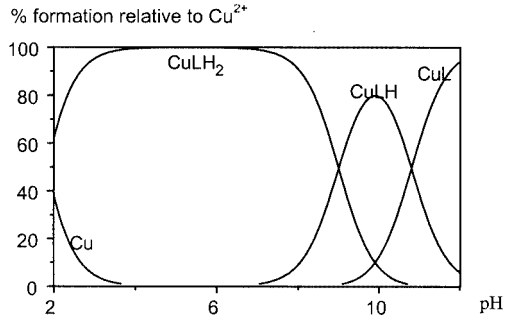

Figure 1. Distribution curves for the mononuclear (*para*cyclen)copper(II) complexes (R = [ligand]/[metal] > 1)

with the three bis(macrocycles) are in the same range as those of complexes CuL^{2+} formed with cyclen or cyclam. Similarly, we observe that the values of the logarithms of the constants β_{210} of the dinuclear complexes Cu_2L^{4+} are twice as high as those of the CuL^{2+} complexes. As a result, the two macrocyclic cavities of the ligands indeed seem to be independent of one another with regard to the complexation phenomenon. Lastly, in the case of mononuclear complexes formed with the *para*cyclam-cyclen ligand, the ESR spectra and the values of the stability constants of the complexes do not allow us to locate the metallic cation in the cyclen or cyclam cavity.

For each ligand, the electronic spectra of solutions with different ratios (R = 2, 1, and 0.5) were plotted between pH = 2 and 11. For the *para*cyclen and *para*cyclam ligands, the spectra of the mono- and dinuclear complexes each show only one absorption band, the position of which remains unchanged whatever the pH may be.

In the case of *para*cyclen, the band is located at a wavelength (λ = 594 nm) very close to that noted for the complex $[Cu(cyclen)(H_2O)]^{2+}$ (λ = 599 nm).[20] The geometries of the complexes formed with cyclen and *para*cyclen are identical; they are pentacoordinated complexes with square-base-pyramidal geometries. The four nitrogen atoms of the macrocycle form the base of each pyramid, whereas a water molecule occupies the fifth position.[19]

For the complex formed with *para*cyclam, the position of the band (λ = 528 nm) is similar to those in complexes formed with different ligands derived from cyclam (512 nm

$< \lambda <$ 550 nm).[19,21] This value is typical of the square-planar CuN_4 chromophore with a strong ligand field.[22] However, the 14-membered cyclam has a ring large enough to surround a range of metal ions, and its complexes generally adopt the strain-free, thermodynamically more stable *trans*-III (*R*,*S*,*S*,*R*) conformation, in which the metal ion is indeed inside the ring of the macrocycle in a square-planar structure, with two adjacent NH hydrogen atoms directed towards one side of the macrocycle plane and the other two in the opposite direction.[23]

In the case of the *para*cyclam-cyclen ligand, the spectra obtained for the dinuclear complex Cu_2L^{4+} ($R < 1$) show only one wide band at $\lambda = 578$ nm, a position intermediary between those noted for the cyclam and cyclen complexes. The spectrum calculated as the sum of the spectra of the *para*cyclen and *para*cyclam complexes also presents an absorption maximum at 578 nm. When the ratio *R* increases, the position of the band changes (Figure 2). The formation of the complexes was monitored by addition of *para*cyclam-cyclen to a solution of copper ions (10^{-3} mol·L^{-1}). For the addition of ligand quantity greater than the quantity of copper ions, the position of the absorption maximum moves closer to $\lambda = 540$ nm and the ESR spectrum is characteristic of a mononuclear species. This value of the absorption maximum indicates that the copper ion is mostly engaged in the cyclam cavity.

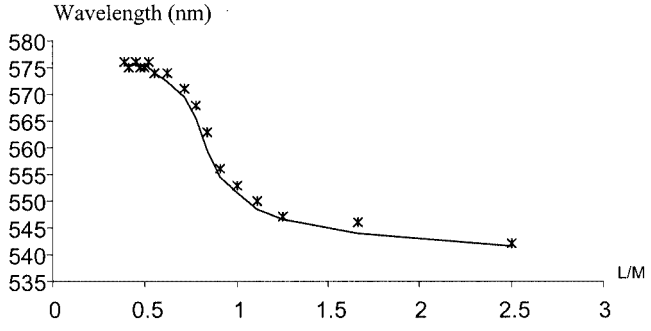

Figure 2. Variation of the wavelength of the maximum of absorbance as a function of the ratio R = L/M in acidic medium (pH ≈ 2); L = *para*cyclam-cyclen, M = Cu; [Cu^{2+}] = 10^{-3} mol·L^{-1}

Solid Complexes Studies

Only dinuclear complexes have been isolated in the solid state. When the ligand was a hydrochloride salt (*para*cyclam and *para*cyclam-cyclen), chloride anions were present in the solid complex. Only *para*cyclen complexes have been obtained as monocrystals suitable for X-ray diffraction. Conversely, structures of monocyclen compounds are scarce.

X-ray Diffraction Studies

(*para*cyclen)$Cu_2(ClO_4)_4$·$4H_2O$

The structure of Cu_2L^{4+} moieties is given in Figure 3, structural data in Table 4, and interatomic distances and angles in Table 5.

Figure 3. ORTEP drawing of the cation [(*para*cyclen)Cu_2]$^{4+}$

The two five-coordinate copper ions are located in square-pyramidal coordination environments. The base is formed by the four nitrogen atoms of the tetraazamacrocycle and an H_2O molecule is bonded in apical position. The two metal centres are always located on each side of the planar xylylene spacer so that the intramolecular Cu−Cu distance is the greatest (Scheme 2).

The Cu^1-N distances, in the 2.020−2.052 Å range generally found for $Cu-N_{amine}$ coordination bonds, and the $N-Cu^1-N$ (85.8−86.8°) and O^1-Cu^1-N angles (101.5−107.5°) indicate geometry close to an ideal square-pyramidal coordination environment for the first copper cation. The Cu^2-N distances (2.006−2.068 Å) and the O^2-Cu^2-N angles (98.2−111.6°), however, indicate a slight distortion of the square-pyramidal geometry. For the two copper ions, $Cu-N_{substituted}$ bonds ($Cu-N^4$ and $Cu-N^5$) are slightly longer than the other $Cu-N_{amine}$ values, as is generally observed.

The monoclinic cell contains four Cu_2L^{4+} moieties (Figure 4), which are stacked with the xylylene groups along an axis, the dihedral angle between two xylylene planes being nearly 90°. We can also note that the copper atoms appear in straight lines. Two neighbouring Cu_2L^{4+} moieties are perpendicular, the tops of the two square-pyramidal moieties point in opposite directions (Scheme 3); this molecular stacking produces intermolecular Cu−Cu distances (9.352, 7.993, or 6.059 Å) shorter than the intramolecular distance (11.540 Å) (Scheme 2). A complete stacking pattern (Figure 4) suggests that hydrogen bonds exist between water molecules, perchlorate ions and amine groups and thus stabilize the crystal lattice of the complex.

[(*para*cyclen)Cu_2]$_2$$(SCN)_8$·$7H_2O$

The structure of the polymeric chain is given in Figure 5, structural data in Table 4, and interatomic distances and angles in Table 6.

The chain is made up of Cu_2L^{4+} moieties linked by a bidentate thiocyanate anion. The terminal S and N donor atoms are coordinated in apical positions, taking the place of the water molecule present in the monomer complex. The copper atom is five-coordinate, and two alternating kinds of Cu_2L^{4+} moieties are present in the chain, the first with two N_4S chromophores (copper atom denoted Cu^1) and the second with two N_5 chromophores (copper atom denoted Cu^2). The Cu^2-N_{SCN} and Cu^1-S distances are 2.054 and 2.482 Å, respectively. The thiocyanate is collinear with the

Table 4. Crystal data and details of the structure determination of (*para*cyclen)$Cu_2(ClO_4)_4{\cdot}4H_2O$ and $[(para\text{cyclen})Cu_2]_2(SCN)_8{\cdot}7H_2O$

	(*para*cyclen)$Cu_2(ClO_4)_4{\cdot}4H_2O$	$[(para\text{cyclen})Cu_2]_2(SCN)_8{\cdot}7H_2O$
Empirical formula	$C_{24}H_{54}N_8O_{20}Cl_4Cu_2$	$C_{56}H_{106}N_{24}O_7S_8Cu_4$
Formula mass	1043.63	1738.3
Temperature [K]	173	173
Crystal system	monoclinic	triclinic
Space group	*P*21/c	$P\bar{1}$
Colour	blue	blue
a [Å]	14.4414(2)	10.5352(3)
b [Å]	28.8197(5)	13.9086(4)
c [Å]	10.5005(2)	14.2432(5)
α [°]	90	78.037(5)
β [°]	110.184(5)	71.201(5)
γ [°]	90	87.741(5)
Volume [Å^3]	4101.9(1)	1932.0(1)
Z	4	1
$D_{calcd.}$ [g·cm^{-3}]	1.69	1.49
Absorption coefficient [mm^{-1}]	1.384	1.366
F(000)	2160	910
λ(Mo−K_α) [Å]	0.71073	0.71073
No of independent reflections	9356	8778
No of reflections [$I > 3.0\sigma(I)$]	4592	5292
*R*1	0.057	0.054
*wR*2	0.070	0.074
Goodness-of-fit on F^2	1.046	1.050

Table 5. Bond lengths [Å] and angles [°] in the (*para*cyclen)-$Cu_2(ClO_4)_4{\cdot}4H_2O$ complex

Cu1−O1	2.189(5)	O1−Cu1−N1	101.5(2)
Cu1−N1	2.020(6)	O1−Cu1−N2	103.9(2)
Cu1−N2	2.021(6)	O1−Cu1−N3	107.5(2)
Cu1−N3	2.018(6)	O1−Cu1−N4	105.2(2)
Cu1−N4	2.052(5)	N1−Cu1−N2	86.8(2)
Cu2−O2	2.139(5)	N1−Cu1−N3	85.8(2)
Cu2−N5	2.068(5)	N1−Cu1−N4	153.3(2)
Cu2−N6	2.006(6)	N2−Cu1−N3	148.5(2)
Cu2−N7	2.028(6)	N2−Cu1−N4	86.4(2)
Cu2−N8	2.025(6)	N3−Cu1−N4	86.6(2)
		O2−Cu2−N5	107.6(2)
		O2−Cu2−N6	111.6(2)
		O2−Cu2−N7	98.2(2)
		O2−Cu2−N8	99.3(2)
		N5−Cu2−N6	86.7(2)
		N5−Cu2−N7	86.2(2)
		N5−Cu2−N8	152.9(3)
		N6−Cu2−N7	150.1(3)
		N6−Cu2−N8	86.5(3)
		N7−Cu2−N8	86.5(3)

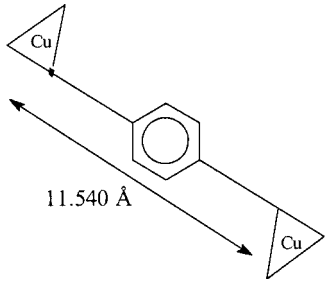

Scheme 2. Intramolecular Cu−Cu distance

Cu−N apical bond and practically perpendicular (93.7°) to the Cu−S apical bond. The Cu−N_{cyclen} distances, in the 2.021−2.059 Å range, and the angles around the copper ion indicate a regular geometry around the metal centre. The polymerisation does not affect the packing of the Cu_2L^{4+} moieties; the intramolecular Cu−Cu distances (11.575 Å) are very close to those observed in the monomer (11.539 Å) and the distance between the two copper ions bridged by the thiocyanate anion (5.810 Å) is also very close to the shortest intermolecular distance obtained in the monomer (6.061 Å). The crystal packing is stabilized by the uncoordinated thiocyanate ion and crystallization water molecules.

X-ray Absorption Spectroscopy (XAS)

The lack of single crystals of (*para*cyclam)Cu_2 and (*para*-cyclam-cyclen)Cu_2 complexes, and their poor crystallinity, prevented from obtaining structural information by the common X-ray diffraction techniques. We therefore decided to study the X-ray absorption near-edge structure (XANES) and the extended X-ray absorption fine structure (EXAFS) spectra of these two compounds with the (*para*cyclen)Cu_2 complex as a model. To the best of our knowledge, the use of XAS techniques in the structural study of bis-(macrocyclic) compounds is new. Only a few uses of XAS for (monocyclam)copper(II) complexes have been reported.[24,25]

A comparison of the XANES spectra for the compounds and the reference [(*para*cyclen)Cu_2 complex] is shown in Figure 6a, with the corresponding first derivatives in Figure 6b. The three spectra seem almost identical with respect to their shape and transition energies. They are typical of copper(II) complexes, each with a very weak 1s→3d pre-

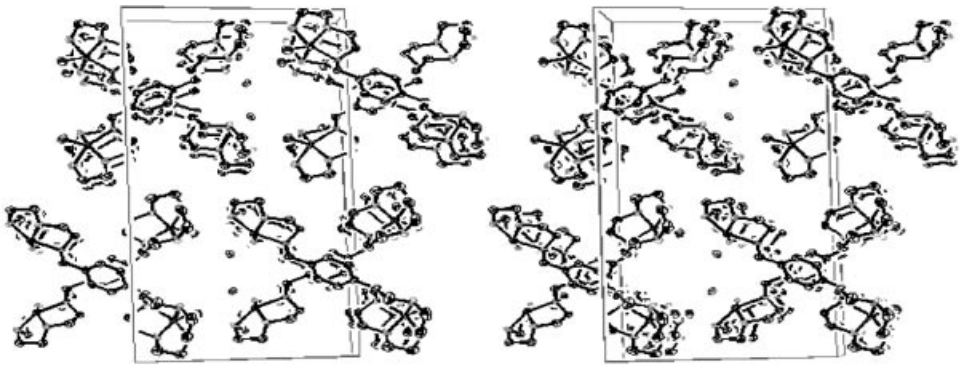

Figure 4. Crystal packing of the unit cell of $[(para\text{cyclen})Cu_2]^{4+}$

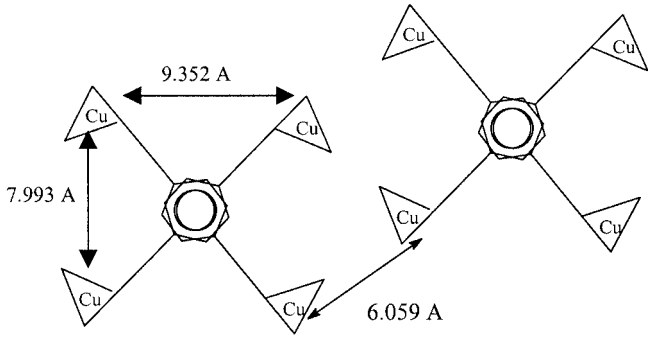

Scheme 3. Intermolecular Cu−Cu distances

edge feature and an absorption edge centred around 8990 eV. Furthermore, each spectrum has the characteristic shoulder (α) of copper(II) in elongated tetragonal surroundings on the low-energy side of the edge.[26] The energy gap between this shoulder (α) and the pre-edge (β) is equal to 6.5 eV for (*para*cyclen)Cu_2 and 6.9 eV for (*para*cyclam)Cu_2. For the (*para*cyclam-cyclen)Cu_2 complex, we can observe a small shoulder on the β peak of the first derivative, and the gaps between α and these two "peaks" are equal to 6.5 and 6.9 eV, which confirms that the copper(II) ion is held in two different geometries arising from the two macrocyclic cavities (cyclam and cyclen). Indeed, the copper(II) ion is in a C_{4v} square-pyramidal environment in the cyclen macrocyclic cavity, and in an O_h or D_{4h} geometry in the cyclam.

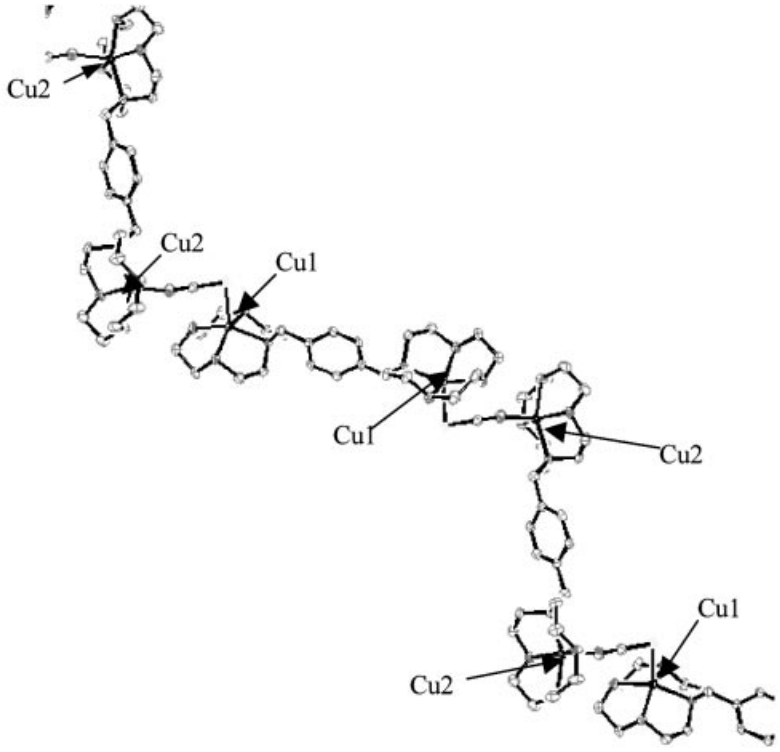

Figure 5. ORTEP drawing of the crystallographic repeating unit of the polymeric chain $[(para\text{cyclen})Cu_2]_2(SCN)_8 \cdot 7H_2O$

Table 6. Bond lengths [Å] and angles [°] in [(*para*cyclen)Cu_2]$_2$(SCN)$_8$·7H_2O

Cu1−N1	2.059(4)	N1−Cu1−N2	86.5(2)
Cu1−N2	2.029(5)	N1−Cu1−N3	150.9(2)
Cu1−N3	2.033(4)	N1−Cu1−N4	85.8(2)
Cu1−N4	2.035(4)	N2−Cu1−N3	85.5(2)
Cu1−S1	2.482(5)	N2−Cu1−N4	147.1(2)
Cu2−N5	2.055(4)	N3−Cu1−N4	85.8(2)
Cu2−N6	2.021(4)	S1−Cu1−N1	106.0(2)
Cu2−N7	2.023(5)	S1−Cu1−N2	100.6(2)
Cu2−N8	2.040(4)	S1−Cu1−N3	102.9(2)
Cu2−N9	2.054(5)	S1−Cu1−N4	112.2(2)
C25−N9	1.172(7)	N5−Cu2−N6	85.4(2)
S1−C25	1.646(6)	N5−Cu2−N7	150.6(2)
		N5−Cu2−N8	86.(2)
		N6−Cu2−N7	85.4(2)
		N6−Cu2−N8	147.2(2)
		N7−Cu2−N8	86.4(2)
		N5−Cu2−N9	107.8(2)
		N6−Cu2−N9	104.0(2)
		N7−Cu2−N9	101.6(2)
		N8−Cu2−N9	108.7(2)
		Cu1−S1−C25	93.7(5)
		Cu2−N9−C25	162.3(5)
		N9−C25−S1[a]	178.8(6)

[a] The bridging NCS^- is indexed N9−C25−S1.

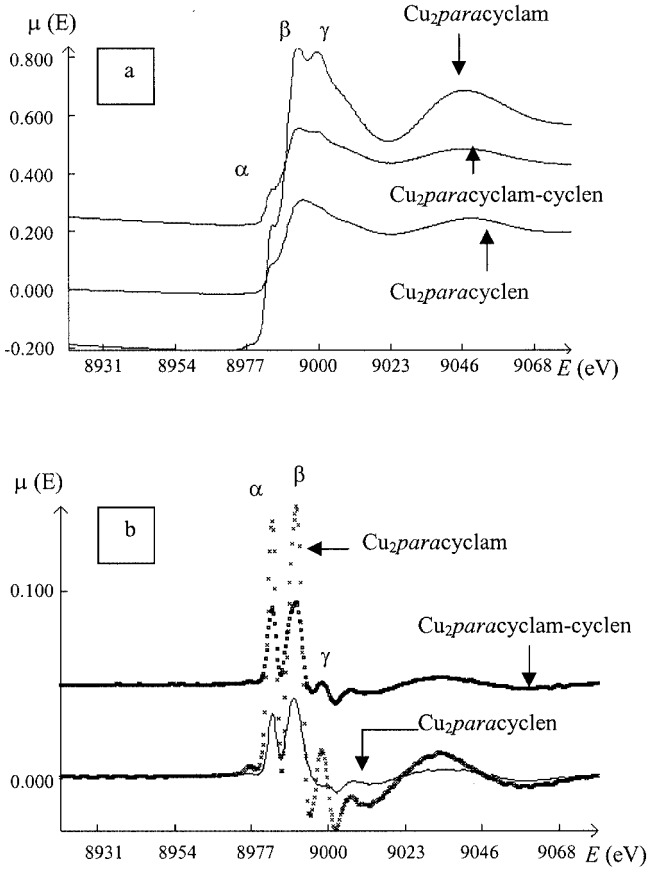

Figure 6. (a) Normalised XANES spectra (pre- and near-edge region) of (*para*cyclam)Cu_2, (*para*cyclam-cyclen)Cu_2, and (*para*cyclen)Cu_2; (b) comparison of their first derivatives

This value provides an estimate for the destabilisation of the $4p_z$ metal orbital, z being the elongation axis.[26,27] Our values are smaller than those (between 8 and 9 eV) found for copper(II) complexes in which the axial ligands are remote from the metal centre, giving rise to a D_{4h} square-planar environment.[27,28] These results are consistent with a distorted octahedral geometry for (*para*cyclam)Cu_2, and a mixed distorted octahedral-square-pyramidal one for (*para*cyclam-cyclen)Cu_2. The main transition, termed β, is attributed to the $1s\rightarrow4p_\pi$ transition, and is mainly affected by axial ligands as discussed above. On the other hand, the γ transition, corresponding to the $1s\rightarrow4p_s$ transition, is mainly sensitive to the equatorial ligands. This transition, centred at 8998 eV in the three compounds, indicates that the bond strengths between central metal ion and ligands are identical, and can be estimated from the (*para*cyclen)Cu_2 reference at approximately 2.35 Å.

The *k*-space experimentally determined and fitted EXAFS spectra $k\chi(k)$ vs. k for (*para*cyclam)Cu_2 and (*para*cyclam-cyclen)Cu_2, at the copper *K*-edge, and the corresponding Fourier transforms are given in Figure 7.

The two experimentally determined $k\chi(k)$ values and their Fourier transforms (FTs) are very similar, and allow us to assume that the local structures of the Cu^{II} ions are nearly the same. The slight differences can be attributed to the size of the macrocyclic cavity, which is greater for cyclam (ten carbon atoms) than for cyclen (eight carbon atoms). Actually, the two (*para*cyclam)Cu_2 and (*para*cyclam-cyclen)Cu_2 compounds differ only by one macrocyclic cavity. The amplitudes of the EXAFS oscillations appear nearly unchanged, indicating the almost identical numbers of nearest neighbours around each metal ion. The Fourier transform spectra are composed of three main peaks. From the expected structures for these complexes, it can be proposed that the first peak should correspond to the four nitrogen atoms of the macrocyclic cavity, and the second to one or two axial water oxygen atoms. The third peak, above 2.7 Å, should correspond to the eight or ten carbon atoms belonging to the cyclen or cyclam cavity.

The number and postulated nature of neighbours, the inter-neighbour distances, the Debye−Waller factors, and the energy threshold resulting from quantitative analysis of EXAFS data for the three first coordination shells of the (*para*cyclam)Cu_2 and (*para*cyclam-cyclen)Cu_2 compounds at the copper *K*-edge are given in Table 7.

The goodness of fit from the fits of the EXAFS functions and the corresponding FTs can be seen in Figure 7. For the (*para*cyclam)Cu_2 complex, the first shell was best fit with four nitrogen atoms per copper(II) ion at an average distance of 2.02 Å from the absorbing copper atom. These four atoms are positioned in the equatorial plane of a Jahn−Teller distorted, elongated octahedron. Actually, the two axial oxygen atoms, of water molecules, of the octahedron are found at 2.78 Å from the Cu^{II} ions, similarly to the arrangement described for $Cu(OH)_2$.[29] The third shell of neighbouring atoms was best fitted with ten carbon atoms at an average distance of 3.12 Å. Taking these values into account, the most likely structural interpretation is that

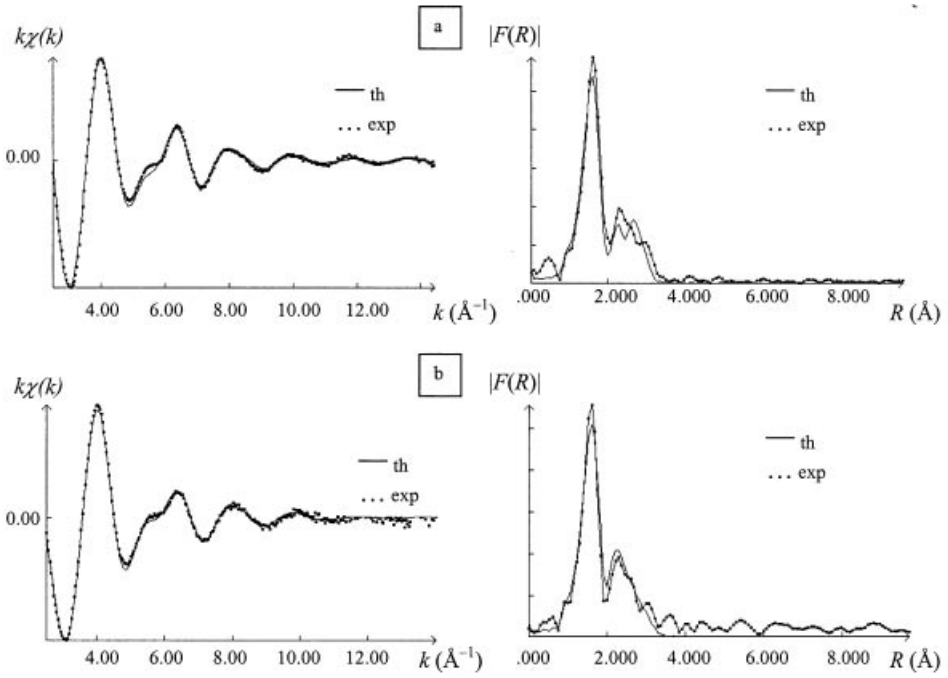

Figure 7. Experimentally measured and fitted k^3-weighted EXAFS spectra and the corresponding Fourier transforms of (*para*cyclam)Cu_2 (a) and (*para*cyclam-cyclen)Cu_2 (b)

Table 7. EXAFS results at the Cu-*K*-edge for the (*para*cyclam)Cu_2 and (*para*cyclam-cyclen)Cu_2 complexes

		N	*R* [Å]	σ [Å^{-1}]	ΔE_0 [eV]
(*para*cyclam)Cu_2	Cu−N	4	2.02	0.023	0.15
	Cu−O	2	2.78	0.007	0.02
	Cu−C	10	3.12	0.055	0.83
(*para*cyclam-cyclen)Cu_2	Cu−N	4	2.04	0.016	0.42
	Cu−O_{cyclam}	2	2.72	0.010	1.02
	Cu−O_{cyclen}	1	2.24	0.068	0.24
	Cu−C_{cyclam}	10	3.13	0.070	0.67
	Cu−C_{cyclen}	8	2.77	0.148	5.61

the two cyclam macrocyclic cavities are located in the equatorial plane with all four nitrogen donor atoms involved in chelating and remaining water of hydration of the first coordination sphere occupying axial positions. This structure agrees well with Ohtaka and Seki's findings[24] for the (monocyclam)copper(II) complex in solution by SAX (Cu−N and Cu−O bond lengths were found to be 2.01 and 2.77 Å), and also those of Tasker and Sklar[30] for the same complex by X-ray diffraction (Cu−N 2.02 Å, distorted octahedral geometry).

Fitting of the EXAFS data for the first coordination shell of the (*para*cyclam-cyclen)Cu_2 complex resulted in a very slight increase in the Cu−N bond length from 2.02 to 2.04 Å. This is consistent with the size of the macrocyclic cavities. Actually, in the cyclam one, the copper(II) ion is in the same plane as the four nitrogen atoms (*trans* N−Cu−N angle around 180°),[31] whereas in the cyclen cavity the metal ion is slightly above (Table 5: *trans* N−Cu−N angle around 150°), increasing the Cu−N bond length. The second and third shells of (*para*cyclam-cyclen)Cu_2 have been fitted for both cyclen and cyclam cavities. The results obtained for the latter are the same as in the (*para*cyclam)Cu_2 complex. For the cyclen cavity the results agree with our X-ray crystallographic data for (*para*cyclen)$Cu_2(ClO_4)_4{\cdot}4H_2O$. However, the more distant carbon atoms give rise to high thermal disorder with a high Debye−Waller factor for these atoms (around 0.15 Å^{-1}). In summary, XAS techniques have been shown to be a good alternative to X-ray diffraction for obtaining structural and geometrical information.

ESR Experiments

The frozen aqueous solution ESR spectra (150 K) of mononuclear complexes show the typical four-line patterns expected for coupling of the electron to the 3/2 spin of a copper(II) nucleus. The hyperfine coupling constants and *g* values are very close to those found for the copper complexes with cyclen or cyclam (Table 2, Figure 8).

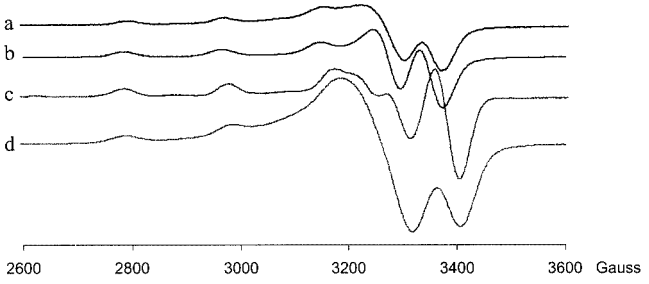

Figure 8. EPR spectra of mononuclear CuL^{2+} complexes at 150 K: (a) (*para*cyclen)Cu, (b) simulation of (*para*cyclen)Cu, (c) (*para*cyclam)Cu, (d) (*para*cyclam-cyclen)Cu

The ESR spectra of the three dinuclear complexes obtained at 150 K in a H_2O/glycerol mixture or in DMF (Figure 9) present a septuplet around 3000 G and a signal at half field, in agreement with those described by Guilard et al.[11] The existence of seven equidistant lines corresponding to the two allowed transitions ($\Delta M_S = 1$) and that of a signal at half field assigned to a forbidden transition ($\Delta M_S = 2$) are characteristic of a dicopper compound with intramolecular exchange between the two copper ions ($I_{Cu} = 3/2$).[32] Unfortunately, the forbidden transition is poorly defined and it is not possible to estimate the Cu−Cu distance from the ratio of the intensity of the forbidden transition to the intensity of the allowed transition.[32]

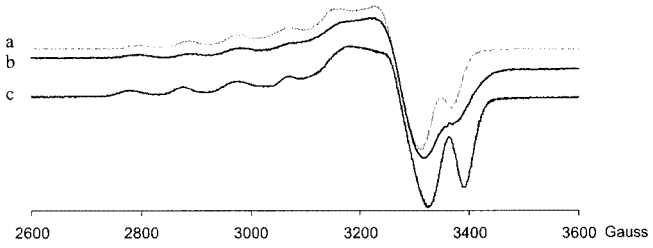

Figure 9. EPR spectra of dinuclear Cu_2L^{4+} complexes at 150 K: (a) (*para*cyclen)Cu_2, (b) (*para*cyclam-cyclen)Cu_2, (c) (*para*cyclam)Cu_2

The *g* values (Table 2) for *para*cyclen and *para*cyclam compounds are similar to those of (cyclen)- and (cyclam)-copper complexes. The hyperfine splittings in the spectra of the dinuclear complexes are approximately half of those characteristic of mononuclear copper(II) complexes in tetragonally distorted octahedral environments for cyclam compounds, and square-pyramidal geometries for cyclen compounds. The $A_{\|}$ values are indicative of a very weak *D* parameter in these dinuclear complexes.[32]

In the dinuclear *para*cyclam-cyclen complex, the copper coordination environment dictated by the macrocyclic holes is different and so the distances between two lines are irregular. However, this effect is insufficient to resolve the two sets of seven lines, the parameters of cyclen and cyclam complexes being too close.

Although the polymeric thiocyanate complex shows two different dinuclear *para*cyclen moieties with CuN_5 and CuN_4S chromophores, respectively, the signal is close to that of (*para*cyclen)$Cu_2(ClO_4)_4$.

Conclusion

In summary, only pure dinuclear complexes were isolated in the solid state. In the case of mononuclear compounds, their isolation was carried out by use of an ion-exchange method with a solution of NaCl as eluent. Unfortunately, sodium chloride could not be completely separated from these complexes.

Among the dinuclear compounds, two complexes formed with the *para*cyclen ligand were obtained as monocrystals suitable for X-ray diffraction. The first is a monomeric compound in which the two five-coordinate copper atoms are located in a square-pyramidal environment (chromophore N_4O), the second, obtained in the presence of an excess of KSCN, is a polymeric chain with two kinds of Cu_2L^{4+} moieties alternately present in the chain (one with two N_4S chromophores, the other with two N_5 chromophores).

With the two other ligands, *para*cyclam and *para*cyclam-cyclen, the complexes were not obtained as monocrystals. They were therefore studied by XAS, which is a good alternative to X-ray diffraction to obtain structural information. In the case of the *para*cyclam ligand, the complex formed is an elongated octahedron (four equatorial N atoms and two axial O atoms of water molecules). With the ligand *para*cyclam-cyclen, the copper atom in the cyclam cavity is six-coordinate (chromophore N_4O_2) and that in the cyclen cavity is five-coordinate (chromophore N_4O).

With regard to the study in solution, the results of the potentiometric titrations, the ESR experiments and the electronic spectra are in good agreement. When the ratio R = ligand/metal is higher than 1, mononuclear complexes $CuLH_n^{(2+n)+}$ ($0 < n < 3$) are formed, and when R is lower than 1, the formation of the dinuclear compounds Cu_2L^{4+} is emphasised. The complexes are very stable and the two macrocyclic cavities of the ligands seem to be independent of one another regarding the complexation phenomenon.

Experimental Section

Spectroscopic Measurements: Electronic spectra in aqueous solution were all measured in the 300−900 nm range with a Lambda 6 Perkin−Elmer spectrophotometer. The ESR spectra were obtained at 150 K with a Bruker ELEXSYS 500 spectrophotometer in the X-band at 9.40 GHz. Simulations were carried out with the software Simfonia.

Potentiometric Measurements: To determine the protonation constants of the ligands and the stability constants of the copper(II) complexes, potentiometric titrations were carried out with an automatic titrator consisting of a Metrohm dosimat 665 microprocessor burette and a Metrohm 713 pH meter connected to a computer. The titration procedure was fully automated.[33] All measurements were performed within a cell thermoregulated at 20.0±0.1 °C under a nitrogen stream to avoid the dissolution of carbon dioxide. the ionic strength was adjusted to 1 with potassium nitrate. The combined type "U" glass electrode Metrohm used had a very low alkaline error. Solutions of ligand (1.10^{-3} to 3.10^{-3} mol·L^{-1}) and ligand/copper nitrate mixture (ligand/metal ratios [L]/[M] in the range 0.5−2) were titrated with a 0.1 mol·L^{-1} KOH solution. The stability constants were calculated and refined with PROTAF.[34] The fitted global formation constants β_{mlh} are defined for the equilibrium (except for the proton, the charges are not shown for clarification):

$$\beta_{mlh} = \frac{[M_m L_l H_h]}{[M]^m [L]^l [H^+]^h}$$

$$m\,M + l\,L + h\,H^+ \rightleftharpoons M_m L_l H_h$$

A negative *h* value refers to the hydroxide ion.

Crystal Structure Determination: The crystal data were collected at 173 K with a Kappa CCD diffractometer using monochromated Mo-K_α radiation (λ = 0.71073Å). The structures were solved by direct methods. After refinement of the non-hydrogen atoms, difference-Fourier maps revealed maxima of residual electron density close to the positions expected for hydrogen atoms. Hydrogen atoms were introduced as fixed contributors at calculated positions [C−H = 0.95 Å; B(H) = 1.3B_{eqv}]. Final difference maps revealed no significant maxima. All calculations used the Nonius OpenMoleN package.[35] Neutral atom scattering factor coefficients and anomalous dispersion coefficients were taken from a standard source.[36] Crystallographic data (excluding structure factors) for the structures reported in this paper have been deposited with the Cambridge Crystallographic Data Centre as supplementary publication nos. CCDC-187962 [(*para*cyclen)$Cu_2(ClO_4)_4$·$4H_2O$] and -187961 {[(*para*cyclen)Cu_2]$_2$$(SCN)_8$·$7H_2O$}. Copies of the data can be obtained free of charge on application to CCDC, 12 Union Road, Cambridge CB2 1EZ, UK [Fax: (internat.) + 44-1223/336-033; E-mail: deposit@ccdc.cam.ac.uk].

X-ray Absorption Data Collection and Processing: The XANES (X-ray absorption near-edge structure) and EXAFS (extended X-ray absorption fine structure) data were collected at the Laboratoire d'Utilisation du Rayonnement Electromagnétique (LURE), Paris-Sud University, with the XAS4 beam line of the storage ring DCI with an energy of 1.85 GeV and a mean intensity of 300−200 mA. The measurements were carried out at the copper *K*-edge in the transmission mode with an Si(111) for EXAFS, and Si(311) for XANES channel-cut monochromator at room temperature. The detector were low-pressure (ca. 0.2 atm) air-filled ionisation chambers. The photon energy was calibrated from the spectrum of a copper foil, 8979 eV being assigned to the pre-edge peak. Each spectrum was the sum of three recordings in the 8830−9830 eV range for EXAFS, and the 8920−9080 eV range for XANES, including the copper *K*-edge (ca. 8979 eV). The XANES spectra were recorded step-by-step, every 0.3 eV with a 2 s accumulation time per point. The spectrum of a 5 μm copper foil was recorded just behind the sample to check the energy calibration, thus ensuring an energy accuracy of 0.25 eV. The EXAFS spectra were recorded with sampling steps of 2 eV, and an integration time of 2.0 s per point was used. The EXAFS data analysis was performed with the "EXAFS pour le Mac" and EXAFS98 programs.[37] The $\chi(k)$ functions were extracted from the data[38] with a linear pre-edge background, a combination of polynomials (of order 5) and spline atomic-absorption background, and normalised by the Lengeler−Eisenberger method.[39] The energy threshold, E_0, was taken at the half maximum of the absorption edge. Radial distribution functions $F(R)$ were calculated by Fourier transforms of $k^3w(k)\mu(k)$ in the 2−14 Å^{-1} range; $w(k)$ is a Kaiser−Bessel apodization window with a smoothness coefficient τ = 3 (k is the photoelectron wavenumber). The peaks corresponding to the successive atomic shells were then isolated and back-Fourier-transformed into k space to determine the mean coordination number N, the bond length R, and the Debye−Waller factor σ by a least-squares fitting procedure using the standard EXAFS formula, without multiple scattering:

$$\chi(k) = S_0^2 \sum_i \left[\frac{N_i}{R_i^2} A_i(k) e^{-2\sigma_i^2 k^2} e^{-2R_i/\lambda(k)} \sin(2kR_i + \Phi_i(k)) \right]$$

The experimental phase $\Phi_i(k,R_i)$ and amplitude $A_i(k,R_i)$ have been extracted from the model compounds of known crystallographic structure, Cu(1,4,8,11-tetraazacyclotetradecane),[24] and (*para*cyclen)Cu_2.

Syntheses: The metal salts were purchased from Aldrich. The other reagents were used as the highest grade commercially available without further purification. The three ligands were synthesized by a new method described by Handel et al.,[40] with an aminal as intermediate.

(*para*cyclen)$Cu_2(ClO_4)_4$·$4H_2O$ (1): The neutral ligand ($5.2\cdot10^{-5}$ mol) was dissolved in distilled water (10 mL) and a copper(II) perchlorate solution in ethanol ($1.17\cdot10^{-4}$ mol) was added dropwise. The blue solution was stirred at room temperature for 7 d and was then concentrated under vacuum. The violet solid was washed twice with absolute ethanol. The complex was recrystallized from saturated aqueous $NaClO_4$ solution. $C_{24}H_{54}Cl_4Cu_2N_8O_{20}$ (1043.1): calcd. C 27.61, H 5.18, N 10.74; found C 27.55, H 5.20, N 10.26.

(*para*cyclam)$Cu_2Cl_2(ClO_4)_2$·H_2O (2): Solid NaOH ($1.75\cdot10^{-3}$ mol) was added to a suspension of ligand hydrochloride ($8.2\cdot10^{-5}$ mol) in absolute ethanol (10 mL). After elimination of NaCl and NaOH in excess, a copper(II) perchlorate solution in methanol ($1.74\ 10^{-4}$ mol) was added dropwise in order to obtain 60 mL of a mauve solution. After stirring at room temperature for 24 h, the blue mauve solid was filtered and washed twice with ethanol. $C_{28}H_{56}Cl_4Cu_2N_8O_9$ (917.1): calcd. C 37.37, H 6.01, N 12.41; found C 36.98, H 6.22, N 12.35.

(*para*cyclam-cyclen)$Cu_2Cl_2(ClO_4)_2$·$2H_2O$ (3): This complex was prepared by the same procedure as used for compound **2**. $C_{26}H_{54}Cl_4Cu_2N_8O_{10}$ (907.1): calcd. C 34.10, H 5.95, N 12.35; found C 34.41, H 6.00, N 11.79.

(*para*cyclen)$Cu_2(SCN)_4$·H_2O (4): After the neutral ligand ($2\cdot10^{-4}$ mol) had been dissolved in methanol (50 mL), an aqueous solution of copper nitrate ($4.2\cdot10^{-4}$ mol) was added. The solution was heated at reflux for 1 h and the solvents were evaporated under vacuum. The crude solid was dissolved in water and a blue solid was precipitated with an excess of KSCN. This solid was filtered and washed with ethanol. $C_{28}H_{48}Cu_2N_{12}O_1S_4$ (823.1): calcd. C 40.72, H 6.06, N 20.36 found C 41.13, H 5.75, N 20.01. Attempted recrystallization in water with an excess of KSCN produced another compound [(*para*cyclen)Cu_2]$_2$$(SCN)_8$·$7H_2O$, a monocrystal suitable for X-ray study.

Synthesis of Mononuclear Complexes: These complexes were very difficult to isolate because of the presence of small amounts of dinuclear compounds or uncomplexed ligands. The isolation of mononuclear compounds could be carried out with an ion-exchange column (SP Sephadex C 25)[41] and an NaCl solution ($0.4\cdot mol\cdot L^{-1}$) as eluent. Unfortunately, sodium chloride could not be completely separated from the complexes.

Acknowledgments

We thank Dr. A. De Cian (Université Louis Pasteur, Strasbourg, France) for the single-crystal X-ray analyses. The Region Champagne-Ardenne is acknowledged for a grant to M. S.

[1] T. A Kaden, *Coord. Chem. Rev.* **1999**, 190−192; T. A Kaden, *Coord. Chem. Rev.* **1999**, 371−389.
[2] M. S. Young, J. J. Chen, *J. Am. Chem. Soc.* **1995**, *117*, 10577−10578.
[3] P. A. Vigato, S. Tamburini, D. E. Fenton, *Coord. Chem. Rev.* **1990**, *106*, 25−170.
[4] [4a] *Copper Coordination Chemistry: Biochemical and Inorganic*

Perspectives (Eds. K. Karlin, J. Zubieta), Academic Press, New York, **1983**. [4b] *Biological and Inorganic Copper Chemistry, vol. I and II perspectives* (Eds. K. Karlin, J. Zubieta), Academic Press, New York, **1986**.
[5] G. J. Bridger, R. T. Skerlj, S. Padmanabhan, S. A. Martellucci, G. W Henson, M. J. Abrams, H. C. Joao, M. Witvrouw, K. De Vreese, R. Pauwels, E. De Clercq, *J. Med. Chem.* **1996**, *39*, 109−119.
[6] E. De Clercq, *Mol. Pharmacol.* **2000**, *57*, 833−839.
[7] K. De Vreese, V. Kofler-Mongold, C. Leutgeb, V. Weber, K. Vermeire, S. Schacht, J. Anne, E. De Clercq, R. Datema, G. Werner, *J. Virol.* **1996**, *70*, 689−696.
[8] E. Kimura, M. Kikuchi, H. Kitamura, T. Koike, *Chem. Eur. J.* **1999**, *5*, 3113−3123.
[9] D. Chartres, L. F. Lindoy, G. V. Meehan, *Coord. Chem. Rev.* **2001**, 216−217; D. Chartres, L. F. Lindoy, G. V. Meehan, *Coord. Chem. Rev.* **2001**, 249−286.
[10] M. Ciampolini, L. Fabbrizzi, A. Poggi, B. Seghi, F. Zanobini, *Inorg. Chem.* **1987**, *26*, 3527−3533.
[11] S Brandes, C. Gros, F. Denat, P. Pullumbi, R. Guilard, *Bull. Soc. Chim. Fr.* **1996**, *133*, 65−73.
[12] R. Schneider, A. Riesen, T. Kaden, *Helv. Chim. Acta* **1986**, *69*, 53−61.
[13] A. McAuley, S. Subramanian, M. J. Zaworotko, K. Biradha, *Inorg. Chem.* **1999**, *38*, 5078−5085.
[14] H. Elias, *Coord. Chem. Rev.* **1999**, *187*, 37−73.
[15] L. Siegfried, A. Urfer, T. A. Kaden, *Inorg. Chim. Acta* **1996**, *251*, 177−183.
[16] Q. Xu, M. Du, R.-H. Zhang, H.-Y. Shen, X.-H. Bu, W.-M. Bu, *Chinese J. Chem.* **2000**, *18*, 357−363.
[17] A. Bianchi, M. Micheloni, P. Paoletti, *Coord. Chem. Rev.* **1991**, *110*, 17−113.
[18] R. D. Hancock, R. J. Motekaitis, J. Mashishi, I. Cukrowski, J. H. Reibenspies, A. E. Martell, *J. Chem. Soc., Perkin Trans. 2* **1996**, 1925−1929.
[19] K. Miyoshi, H. Tanaka, S. Tsuboyama, S. Murata, H. Shimizu, K. Ishizu, *Inorg. Chim. Acta* **1983**, *78*, 23−30.
[20] M. Gaspar, R. Grazina, A. Bodor, E. Farkas, M. A. Santos, *J. Chem. Soc., Dalton Trans.* **1999**, 799−806.
[21] [21a] A. E. Goeta, J. A. K. Howard, D. Maffeo, H. Puschmann, J. A. G. Williams, D. S. Yufit, *J. Chem. Soc., Dalton Trans.* **2000**, 1873−1880. [21b] R. Buxtorf, T. A. Kaden, *Helv. Chim. Acta* **1974**, *57*, 1035−1042. [21c] M. R. Oberholzer, M. Neuburger, M. Zehnder, T. A. Kaden, *Helv. Chim. Acta* **1995**, *78*, 505−513.
[22] B. J. Hathaway, *J. Chem. Soc., Dalton Trans.* **1972**, 1196−1199.
[23] M. T. S. Amorim, S. Chaves, R. Delgado, J. R. Frausto da Silva, *J. Chem. Soc., Dalton Trans.* **1991**, 3065−3071.
[24] H. Ohtaki, H. Seki, *J. Macromol. Sci. Chem.* **1990**, *A27*, 1305−1319.
[25] J. H. Choy, B. W. Kim, J. B. Yoon, J. C. Park, *Mol. Cryst. Liq. Cryst.* **1998**, *311*, 303−311.
[26] N. Kosugi, T. Yokoyama, K. Asakuna, H. Kuroda, *Chem. Phys.* **1984**, *91*, 249−258.
[27] C. Surville-Barland, R. Ruiz, A. Aukauloo, Y. Journeaux, I. Castro, B. Cervera, M. Julve, F. Lloret, F. Sapina, *Inorg. Chim. Acta* **1998**, *278*, 159−169.
[28] C. Mangenay, J. C. Lacroix, K. I. Chane-Ching, M. Jouini, F. Villain, S. Ammar, N. Jouini, P. C. Lacaze, *Chem. Eur. J.* **2001**, *7*, 5029−5040.
[29] M. Magini, *J. Chem. Phys.* **1981**, *74*, 2523−2529.
[30] P. A. Tasker, L. Sklar, *J. Cryst. Mol. Struct.* **1975**, *5*, 329−338.
[31] T. H. Lu, T. H. Tahirov, Y. L. Liu, C. S. Chung, C. C. Huang, Y. S. Hong, *Acta Crystallogr., Sect. C* **1996**, *52*, 1093−1099.
[32] [32a] S. S. Eaton, K. M. More, B. M. Sawant, G. R. Eaton, *J. Am. Chem. Soc.* **1983**, *105*, 6560−6567. [32b] S. S. Eaton, *J. Am. Chem. Soc.* **1982**, *104*, 5002−5003.
[33] I. Déchamps-Olivier, J. P. Barbier, M. Aplincourt, N. Oget, F. Chuburu, H. Handel, *Helv. Chim. Acta* **1999**, *82*, 790−795.
[34] [34a] R. Fournaise, C. Petitfaux, *Talanta* **1987**, *34*, 385−395. [34b] R. Fournaise, C. Petitfaux, *Analysis* **1990**, *18*, 242−249.
[35] OpenMoleN, *Interactive Structure Solutions*, Nonius B. V., Delft, The Netherlands, **1997**.
[36] D. T. Cromer, J. T. Waber, *International Tables for X-ray Crystallography*, The Kyonoch Press, Birmingham, **1974**, vol. IV, tables 2.2b, 2.3.1.
[37] [37a] A. Michalowicz, in: *Logiciels pour la Chimie*, Société Française de Chimie, Paris, **1991**, p. 102. [37b]A. Michalowicz, *J. Chem. Phys. IV* **1997**, *7*, 235−245.
[38] [38a] B. K. Teo, in: *Inorganic Chemistry Concepts, EXAFS: Basic Principles and Data Analysis*, Springer-Verlag, Berlin, **1986**, p. 9. [38b] D. C. Königsberger, R. Prins, in: *X-ray Absorption Principles, Applications, Techniques of EXAFS, SEXAFS and XANES*, John Wiley, New York, **1988**. [38c] F. W. Lytle, D. E. Sayers, E. A. Stern,, *Physica* **1989**, *B158*, 701−704 (“Co-Chairmen Report of the International Workshop on Standards and Criteria in X-ray Absorption Spectroscopy”).
[39] B. Lengeler, P. Eisenberger, *Phys. Rev.* **1980**, *B21*, 4507−4518.
[40] M. Le Baccon, F. Chuburu, L. Toupet, H. Handel, M. Soibinet, I. Déchamps-Olivier, J. P. Barbier, M. Aplincourt, *New J. Chem.* **2001**, 1168−1174.
[41] L. Fabbrizzi, L. Montagna, A. Poggi, T. A. Kaden, L. C. Siegfried, *J. Chem. Soc., Dalton Trans.* **1987**, 2631−2687.

Received September 16, 2002

